Synthesis, spectral, thermal, X-ray single crystal of new RuCl$_2$(dppb)diamine complexes and their application in hydrogenation of Cinnamic aldehyde

Ismail Warad [a],*, Hanan Al-Hussain [a], Rawhi Al-Far [b], Refaat Mahfouz [a], Belkheir Hammouti [c], Taibi Ben Hadda [d]

[a] Department of Chemistry, King Saud University, P.O. Box 2455, Riyadh 11451, Saudi Arabia
[b] Department of Applied Sciences, Faculty of Applied Sciences and I.T., Al-Balqa' Applied University, Salt 19117, Jordan
[c] LCAE-URAC18, Faculté des Sciences, Université Mohammed Ier, B.P. 717, Oujda 60000, Morocco
[d] Laboratoire de Chimie Matériaux, FSO, Université Mohammed Ier, Oujda 60000, Morocco

ARTICLE INFO

ABSTRACT

The preparation of new three trans-[RuCl$_2$(dppb)(N–N)] with mixed diamine (N–N) and 1,4-bis-(diphenylphosphino)butane (dppb) ligands, starting from RuCl$_2$(PPh$_3$)$_3$ as precursor is presented. The complexes are characterized on the basis of elemental analysis, IR, ^{1}H, ^{13}C and ^{31}P{^{1}H}NMR, FAB-MS, TG/DTA and single crystal X-ray diffraction studies. Complex (2L$_1$) crystallizes in the monoclinic unit cells with the space group P2$_1$. The catalysts are evaluated for their Cinnamic aldehyde hydrogenation. The catalysts show excellent activity and selectivity for the unsaturated carbonyl compound under mild conditions.

Introduction

Over the years, phosphine ligands have played a very important role in the design and development of metal complexes-mediated catalysis [1–8]. Among them, diphosphines have received much attention because of their tendency to form more stable complexes than their non chelating phosphine analogs under the harsh reaction conditions required for catalysis [9–13]. Moreover the chelate diphosphine ligands decreased the number of isomers compared to monodentate phosphine ligands which de-complicated the structural identification of synthesized complexes [5–10]. Due to the presence of phosphine atoms in the backbone of the coordinated ligands, structural and fluxional behaviors of such complexes during reaction processes can be easy monitored by ^{31}P{^{1}H} NMR [14]. Although structural and dynamic behaviors of transition metal complexes containing monodentate and bidentate ligands have been often investigated in the last few years, it still remains an active area of research interest [15,16]. In recent years, many ruthenium/diphosphine complexes have been synthesized and characterized for their applications in the field of electrocatalysis, photolysis, bioinorganic chemistry, and asymmetrical catalytic hydrogenation [17–19]. Mixed diamine(phosphine)ruthenium(II) complexes have received much attention in recent years due to their remarkable performance as hydrogen transfer catalysts [8,9] and asymmetric hydrogenation of unsaturated carbonyl compounds [5,6,10]. Exchange of the monodentate phosphine such as triphenylphosphine (PPh$_3$) or ether-phosphine (P–O) ligands and the bidentate phphosphine such as 1,3-bis-diphenylphosphinepropane (dppp) or 1,1-bis(diphenyl-phosphinomethyl)ethene, (dppme) ligands on ruthenium(II) complexes by several types of diamine ligands to synthesize diamines/diphosphine/ruthenium(II) complexes is currently one of our ongoing line of investigations [7–9,14,20,21]. In continuation of our ongoing interest in synthesis and characterization of a variety of novel diamines/diphosphine/ruthenium(II) complexes and their applications [7–9]. Herein, we synthesized and characterized RuCl$_2$(dppb)diamine complexes obtained from 1,4-bis(diphenylphosphino)butane and various aliphatic diamines viz., 1,3-diammnopropane 2-methyl-1,2-ethanediamine, and 1,4-diaminobutane. Complexes of this type proved to be highly selective and effective catalyst in the hydrogenation of carbonyl group of the Cinnamic aldehyde under mild conditions.

Experimental

General remarks, materials and physical measurements

All reactions were carried out in an inert atmosphere (argon) by using standard high vacuum and Schlenk-line techniques.

* Corresponding author. Tel./fax: +966 1 4675992.
  E-mail address: warad@ksu.edu.sa (I. Warad).

1,4-bis(diphenylphophino)butane (dppb), 1,4-diaminobutane, 1,3-diamninopropane and 2-methyldiaminoethane were available from Merck and used as received. $RuCl_2(PPh_3)_3$ were previously prepared in our lab [22]. Elemental analyses were carried out on an Elementar Varrio EL analyzer. High-resolution ^1H, $^{13}C\{^1H\}$, DEPT 135, and $^{31}P\{^1H\}$ NMR spectra were recorded on a Bruker DRX 250 spectrometer at 298 K. FT-IR and FAB-MS data were obtained on a Bruker IFS 48 FT-IR spectrometer and Finnigan 711A (8 kV), modified by AMD and reported as mass/charge (m/z), respectively. The analyses of the hydrogenation experiments were performed on a GC 6000 Vega Gas 2 (Carlo Erba Instrument) with a FID and capillary columns PS 255 [10 m, carrier gas, He (40 k Pa), integrator 3390 A (Hewlett–Packard)].

Synthesis of the RuCl₂(dppb)diamine complexes 2L₁–2L₃

By treating $Cl_2Ru(PPh_3)_3$ with one equivalent amount of dppb ligand in dichloromethane and inert atmosphere the brown color turns directly to green one due to the in situ formation of $RuCl_2$/PPh_3/dppb precursor, this precursor served to prepare 2L₁–2L₃ by treating it with the equivalent amount of 2L₁–2L₃ diamines co-ligand in dichloromethane. The yellow, air sensitive mixed [(diamine)[bis(diphenylphosphino)butane]ruthenium(II)] complexes 2L₁–2L₃ were formed directly in good yields. Even in the presence of excess of diamine ligands only the monodentate PPh₃ ligands were exchanged which facilitated and reduced the synthesized complexes number (Scheme 1).

General procedure for the preparation of complexes 2L₁–2L₃

The corresponding diamine (10% excess of L₁–L₃) was dissolved in 10 mL of dichloromethane and the resultant solution was added dropwise to a stirred solution of (RuCl₂/PPh₃/dppb) precursor in 10 mL of dichloromethane. The reaction mixture was stirred for 1 min. at room temperature under inert atmosphere resulting in the change in color from green to light yellow. The resulting yellow solution was concentrated by vacuum to 1 ml followed by the addition of 30 mL of diethyl ether to cause precipitation of 2L₁–2L₃. The resulting precipitate was collected and re-crystallized from dichloromethane/n-hexane and obtained in analytically pure form.

2L₁: Complex **1** (0.25 g, 0.26 mmol) was treated with dppb ligand (0.11 g, 0.27 mmol), then (0.02 g, 0.27 mmol) of **L₁** diamine ligand was added to give **2L₁**. Yield (90%), yellow crystal, mp. 298 °C. ^1H NMR ($CDCl_3$): ∂ (ppm) 1.82 (m, 4H, $PCH_2C\underline{H}_2$), 2.88 (b, 6H, $C\underline{H}_2CH_2N$, PCH_2), 3.18 (b, 8H, CH_2N, NH_2), 7.19–7.60 (2 m, 20H, C_6H_5), $^{31}P\{^1H\}$($CDCl_3$): ∂ (ppm) 46.87. $^{13}C\{^1H\}$NMR ($CDCl_3$):∂ (ppm) 22.78 (s, $PCH_2C\underline{H}_2$), 26.63 (m, PCH_2), 29.19 (s, $NCH_2C\underline{H}_2$), 39.98 (s, NCH_2), 128.23 (m, m-C_6H_5), 129.36 (s, p-C_6H_5), 133.83 (m, o-C_6H_5), 136.64 (m, i-C_6H_5). FAB-MS; (m/z) 672.1 [M⁺]. Anal.

Found: C, 55.46; H, 5.60; N, 4.27; Cl, 10.64. Calc. for $C_{31}H_{38}Cl_2N_2P_2Ru$: C, 55.42; H, 5.69; N, 4.16; Cl, 10.56%.

2L₂: Complex **1** (0.25 g, 0.26 mmol) was treated with dppb ligand (0.11 g, 0.27 mmol), then (0.02 g, 0.27 mmol) of **L₂** diamine ligand was added to give **2L₂**. Yield (95%), yellow powder, mp. 296 °C. ^1H NMR ($CDCl_3$): ∂ (ppm) 0.91 (d, $^3J_{HH}$ = 6.02 Hz, 3H, CH_3), 1.78 (m, 4H, $PCH_2C\underline{H}_2$), 2.44-2.68 (3b, 10H, PCH_2, NH_2, NCH_2), 3.14, (m, 1H, NCH), 7.22-7.7.55 (2 m, 20H −C_6H_5). $^{31}P\{^1H\}$NMR ($CDCl_3$): ∂ (ppm) 46.87, 2.04 (AB Pattern).$^{13}C\{^1H\}$NMR ($CDCl_3$): ∂(ppm) 19.20, 20.51 (2s, $PCH_2C\underline{H}_2$), 20.54 (s, CH_3), 25.71, 26.18 (2 m, PCH_2),, 49.66 (s, NCH_2), 50.96 (s, NCH), 127.97 (m, m-C_6H_5), 129.11 (s, p-C_6H_5), 133.09 (m, o-C_6H_5), 136.56 (m, i-C_6H_5). FAB-MS; (m/z) 672.1 [M⁺]. Anal. Found: C, 55.34; H, 5.58; N, 4.07; Cl, 10.39. Calc. for $C_{31}H_{38}Cl_2N_2P_2Ru$: C, 55.42; H, 5.69; N, 4.16; Cl, 10.56%.

2L₃: Complex **1** (0.25 g, 0.26 mmol) was treated with dppb ligand (0.11 g, 0.27 mmol), then (0.024 g, 0.27 mmol) of **L₂** diamine ligand was added to give **2L₂**. Yield (55%), Yellow powder, mp. 195 °C. ^1H NMR ($CDCl_3$): ∂(ppm) 0.75 (m, 4H, $\underline{CH}_2CH_2N$), 1.81 (m, 4H, $PCH_2C\underline{H}_2$), 2.78 (b, 6H,$C\underline{H}_2CH_2N$, PCH_2), 3.22 (b, 10H, CH_2N, NH_2), 7.19-7.60 (2 m, 20H, C_6H_5), $^{31}P\{^1H\}$NMR ($CDCl_3$): ∂(ppm) 47.03. $^{13}C\{^1H\}$NMR ($CDCl_3$): ∂ (ppm) 19.97 (s, $PCH_2C\underline{H}_2$), 26.23 (m, PCH_2), 29.02 (s, $NCH_2C\underline{H}_2$), 38.56 (s, NCH_2), 128.20 (m, m-C_6H_5), 129.27 (s, p-C_6H_5), 133.78 (m, o-C_6H_5), 136.57 (m, i-C_6H_5). FAB-MS (m/z), 686.11 [M⁺]. Anal. Found: C, 55.88; H, 5.72; N, 4.17; Cl, 10.41. Calc. for $C_{32}H_{40}Cl_2N_2P_2Ru$: C, 55.98; H, 5.87; N, 4.08; Cl, 10.33%.

General procedure for the catalytic studies

(0.02 mmol) of respective complexes 2L₁–2L₃ and (0.20 mmol) of the co-catalysts (KOH or K2CO3 and (2.0 mmol) of Cinnamic aldehyde are placed together in a 100 mL pressure Schlenk tube. The solid mixture was stirred and warmed during the evacuation process, during that the Schlenk tube was filled and refilled with argon several times to insure the inert atmosphere, 40 mL of 2-propanol was added to the reaction mixture then sonicated for 10 min to complete the dissolving. The mixture was vigorously stirred, degassed by two freeze-thaw cycles, and then pressurized with dihydrogen of 3 bar. The reaction mixture was vigorously stirred at RT for 1 h. During the hydrogenation process samples were taken from the reaction mixture after the gas was removed to control the conversion and turnover frequency. The samples were inserted by a special glass syringe into a gas chromatograph and the kind of the reaction products was compared with authentic samples.

X-ray structural analyses for complexes 2L₁

Crystal of 2L₁ was grown by slow diffusion of diethyl ether into a solution of the complex in dichloromethane. Data were collected at 173(2) Siemens P4 diffractometer operating in the omega scan mode, using graphite monochromated Mo Kα radiation (λ = 0.71 073°A). Details of crystal data, data collection, and structure refinement are given in Table 1. The structure was solved by direct methods using the Bruker SHELXS-97 programme and refined by full matrix least-squares on F^2 using the Bruker SHELXL-97 programme [23,24].

Result and discussion

Ruthenium(II) complexes synthetic investigation

The reason for choosing the C_2-symmetric dppb ligand with two equivalent P atoms was to reduce the number of possible isomeric metal complexes, as well as the number of different
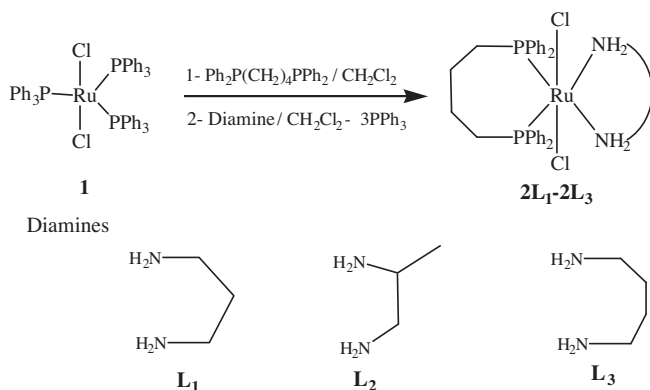
Scheme 1. Synthesis of new Ru(II) complexes.

Table 1
Crystal data and structure refinement for complex **2L$_1$**.

Empirical formula	C$_{31}$H$_{38}$Cl$_2$N$_2$P$_2$Ru
Formula weight	672.54
Temperature	173(2) K
Wavelength	0.71073 Å
Crystal system	Monoclinic
Space group	P 21
Unit cell dimensions	a = 10.0927(15) Å α = 90°
	b = 10.6480(9) β = 100.630(13)°
	c = 14.1523(18) Å γ = 90°
Volume	1494.8(3) Å^3
Z	2
Density (calculated)	1.494 mg/cm^3
Absorption coefficient	0.834 mm^{-1}
F(000)	692.0
Crystal size	0.5 × 0.2 × 0.2 mm^3
Theta range for data collection	2.29–27.50°
Index ranges	−13<=h<=1, −13<=k<=13, −18<=l<=18
Reflections collected	3618
Independent reflections	3618 [R (int) = 0.0240]
Completeness to theta = 27.50°	99.9%
Absorption correction	Numerical
Max. and min. transmission	0.835 and 0.805
Refinement method	Full-matrix least-squares on F^2
Data/restraints/parameters	3618/1/344
Goodness-of-fit on F2	1.049
Final R indices [I>2/s (I)]	R1 = 0.0272, wR2 = 0.0701
R indices (all data)	R1 = 0.0278, wR2 = 0.0705
Absolute structure parameter	0.00(1)
Extinction coefficient	0.0068(7)
Largest diff. peak and hole	0.861 and −1.175 e Å^{3-}

Fig. 1. ^{31}P{^{1}H} NMR spectrum of **2L$_1$** (a) and **2L$_2$** (b) direct dissolved in CDCl$_3$ at RT.

substrate–catalyst arrangements and reaction pathways, when compared with a nonsymmetrical ligand. The reaction scheme for the synthesis of new ruthenium(II) complexes is depicted in Scheme 1. The air-sensitive **2L$_1$–2L$_3$** complexes of the formula *trans*-Cl$_2$Ru(dppb)diamines with three different types of diamine co-ligand were obtained in a very good yield by a substitution reaction starting from Cl$_2$Ru(PPh$_3$)$_3$ (**1**) with one equivalent mole of dppb ligand followed by one equivalent mole of the corresponding diamine co-ligands in dichloromethane. The structure of the desired complexes has been deduced from elemental analysis, infrared spectroscopy, FAB-mass spectrometry, ^{1}H, ^{13}C{^{1}H} and ^{31}P{^{1}H} NMR, spectroscopy TG/DTA, additionally (**2L$_1$**) was subjected to X-ray crystallography.

The stepwise formation of these complexes was monitored by ^{31}P{^{1}H} spectroscopy as well as the color changes.

NMR investigations

The ^{31}P{^{1}H} NMR spectra of the complexes **2L$_1$–2L$_3$** were recorded in CDCl$_3$ immediately after dissolution. It is important to point out that in ruthenium/dppb/diamine complexes, when the P atoms are trans to nitrogen, the ^{31}P{^{1}H}NMR chemical shifts occur around 45 ppm [25–27]. The ^{31}P{^{1}H} NMR spectra of complexes with **2L$_1$** and **2L$_3$** showed only one signal at 46.87 and 47.03 ppm, respectively as in Fig. 1a, as expected for symmetrical arrangements of the P atoms and would be assigned to the formation of *trans*-[Cl$_2$Ru(dppb)(diamine)] complexes with C$_{2v}$ symmetry, where the nitrogen atom is *trans* to the phosphorus atom as in Scheme 1. In case of complex **2L$_2$**, the asymmetric diamine causes a loss of the C$_2$ axis which results in splitting of the ^{31}P resonances into AB pattern with δ (ppm) 46.45, 47.29 (AB pattern, $^2J_{PP}$ = 51.40 Hz). The ^{31}P chemical shifts and the ^{31}P–^{31}P coupling constants are consistent with a *cis* arrangement of the P atoms in dppb (Fig. 1b).

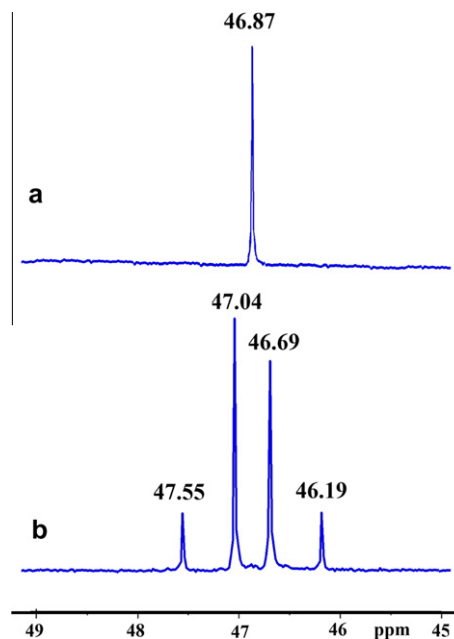The ^{1}H NMR spectra of **2L$_1$–2L$_3$** complexes have been recorded in CDCl$_3$ solution to confirm the binding of the ligands to
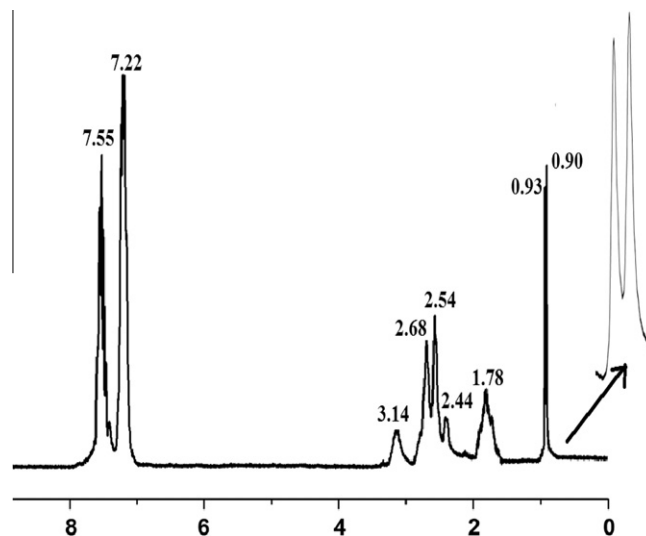

Fig. 2. ^{1}H NMR (ppm) spectrum of **2L$_2$** in CDCl$_3$ at RT.

ruthenium and their assignments are given in Section 2. Several characteristic sets of signals are observed attributed to the dppb and diamine ligands. The integration of the ^{1}H resonances confirms that the dppb to diamine ratio is in agreement with the structural composition of *trans*-[Cl$_2$Ru(dppb)diamine], **2L$_1$–2L$_3$** complexes. The ^{1}H NMR spectra of all the complexes present a set of signals in the region 7.2–7.4 and 1.7–3.3 ppm attributed to aromatic and aliphatic protons, respectively. Additional double signal for –CH$_3$ protons in **2L$_2$** complex is observed at 0.92 ppm (Fig. 2).

The ^{13}C{^{1}H}NMR spectra also corroborate the structure of desired complexes. Characteristic ^{13}C NMR signals due to the carbons in diamine and dppb ligands in all the complexes appeared at their expected positions.

135 dept ^{13}C{^{1}H} NMR spectra, as a typical technique to differentiate the C, CH, CH$_2$ and CH$_3$ carbon types were investigated to identify the structure of desired complexes, typical example of **2L$_1$** and **2L$_2$** complexes was recorded as in (Fig. 3).
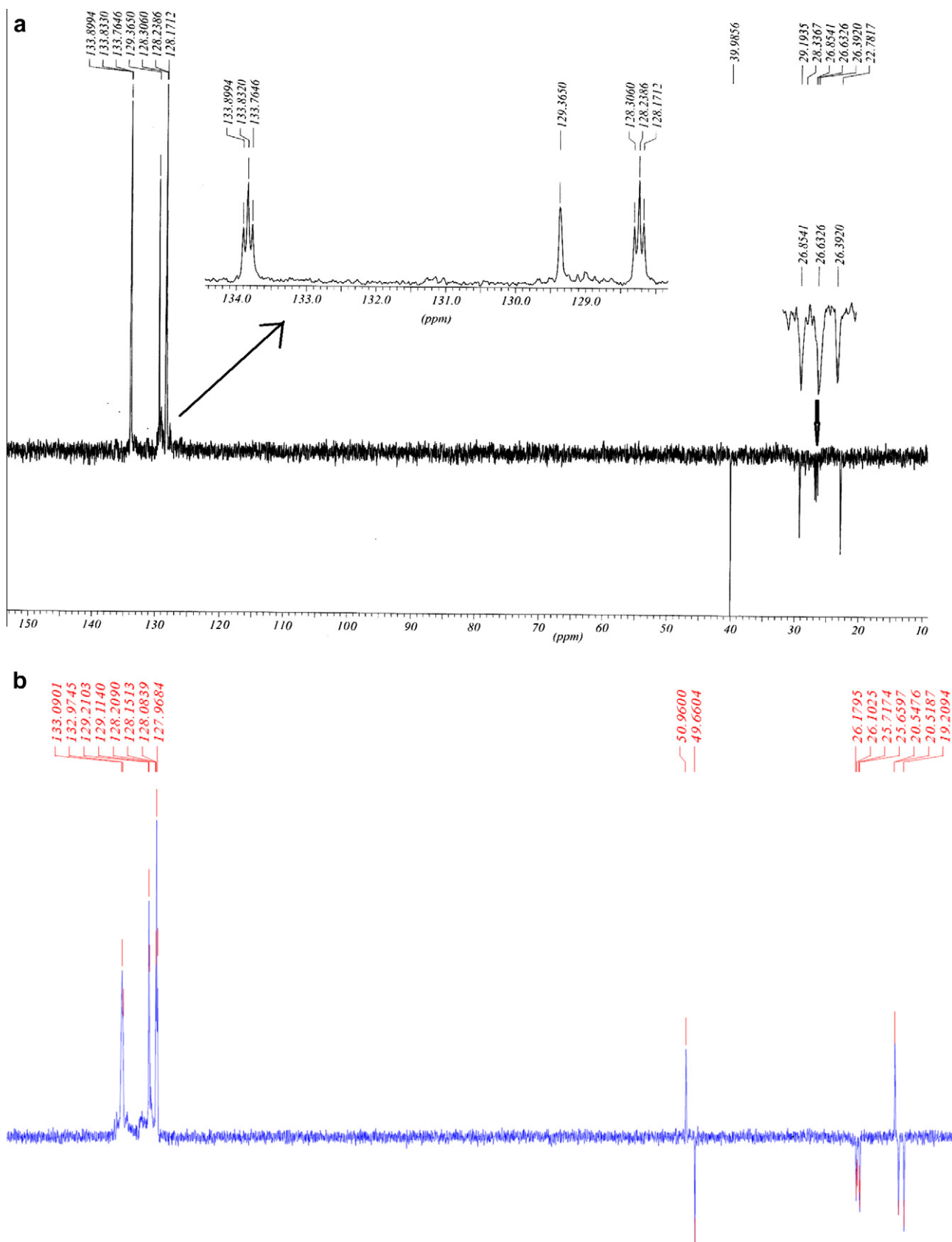
Fig. 3. The 135 Dept $^{13}C\{^1H\}$ NMR spectra (ppm) corroborates the structures of $2L_1$ (a) and $2L_1$ (b).
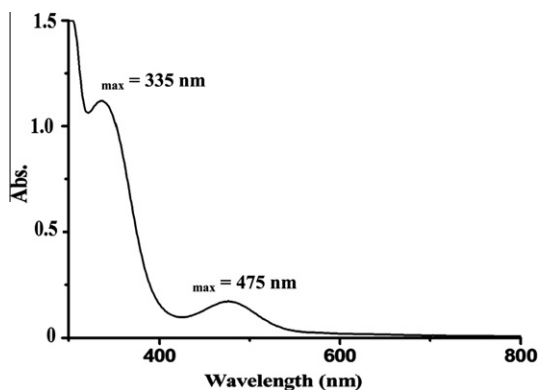
Fig. 4. UV–Vis spectrum of $2L_1$ complex.

Electronic absorption spectral studies

The electronic absorption spectra of $2L_1$–$2L_3$ were acquired in dichloromethane at room temperature. The complexes formed very intense colored solutions and thus very low concentrations have been used (10^{-4} M). Ruthenium(II) complexes usually exhibit intense peaks in the UV region corresponding to ligand based $\pi–\pi^*$ transitions with overlapping metal-to-ligand charge transfer (MLCT) transitions in the visible region [25–27]. An analogous general pattern has been observed in the electronic absorption spectra of complexes under study. The complexes $2L_1$–$2L_3$ displayed intense transitions in the UV–Vis region. On the basis of its intensity and position, the lowest energy transitions in the visible region at 488–430 and 380–330 nm have been tentatively assigned to $M_{d\pi}$–$L_{\pi*}$ metal to ligand charge transfer transitions (MLCT). Bands in the

high-energy side at 200–280 nm have been assigned to intra-ligand $\pi–\pi^*/n–\pi^*$ transitions [25–27]. As typical example absorption bands at 280, 335 and 475 nm of complex $2L_1$ are depicted in Fig. 4.

Mass spectra

Another strong evidence for the structural elucidation comes from the mass spectra. The observed molecular ion peak (s) at m/z 672.1, 672.4 and 687.5 corresponding to complexes $2L_1$–$2L_3$, respectively are consistent with the proposed molecular formula. The FAB-MS spectrum of complex ($2L_1$) shows (Fig. 5) a molecular ion peak $[M^+]$ $m/z = 672.1$ which is corresponding to its molecular formula $[C_{31}H_{38}Cl_2N_2P_2Ru]^+$ parent ion with 100% intensity base peak. The other fragments appeared (Fig. 6) in the spectrum are as $m/z = 637.1$ ($[C_{31}H_{38}ClN_2P_2Ru]^+$, 40%, $[M^+]$-Cl), 584.0 ($[C_{31}H_{38}N_2P_2Ru]^+$, 20%, $[M^+]$-2Cl). It also shows a series of peaks at 222.3, 243.2, 289.2, 387.2, 329.1, 335.1, 355.1, 429.1, 475.1, 548.1 and 511.1.

IR spectral investigations

The IR spectra of the complexes have been examined in comparison with the spectra of the free dppb and diamine ligands. IR spectra of the $2L_1$–$2L_3$ in particular show main four sets of characteristic absorptions in the range 3400–3200, 3190–3000, 2950–2820 and 270–285 cm^{-1}, which can be assigned to –NH$_2$, Ph-CH, alkyl-CH and Ru–Cl stretching vibrations, respectively. All the other functional group vibrations are appeared at their expected positions as in Fig. 7.
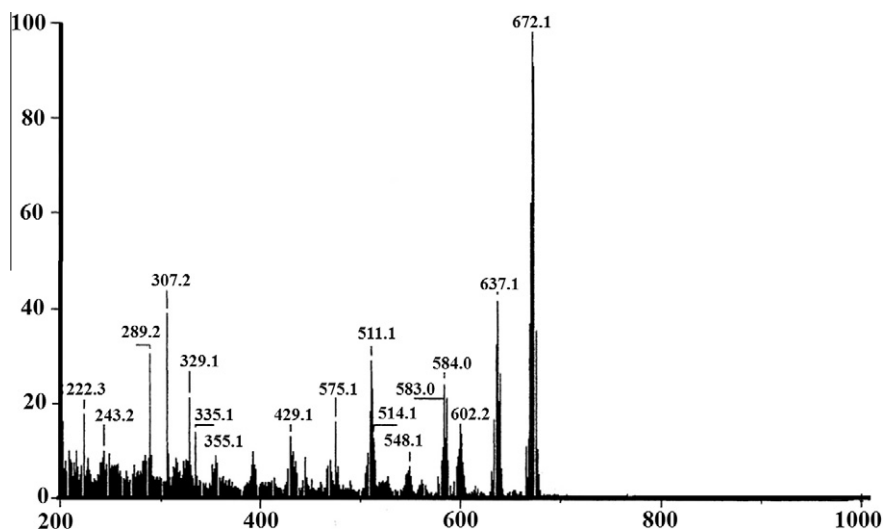

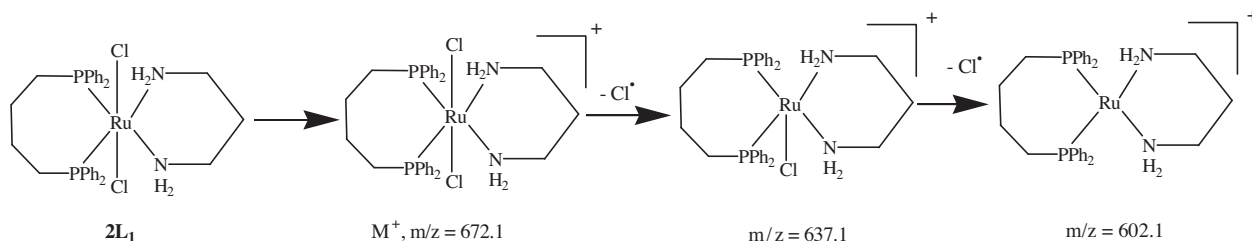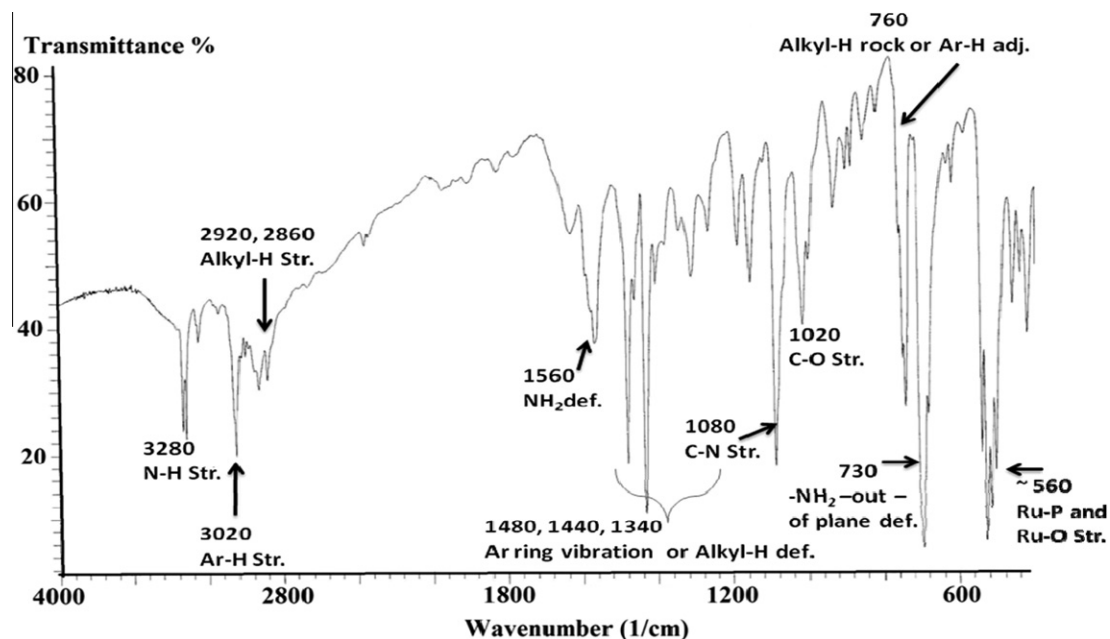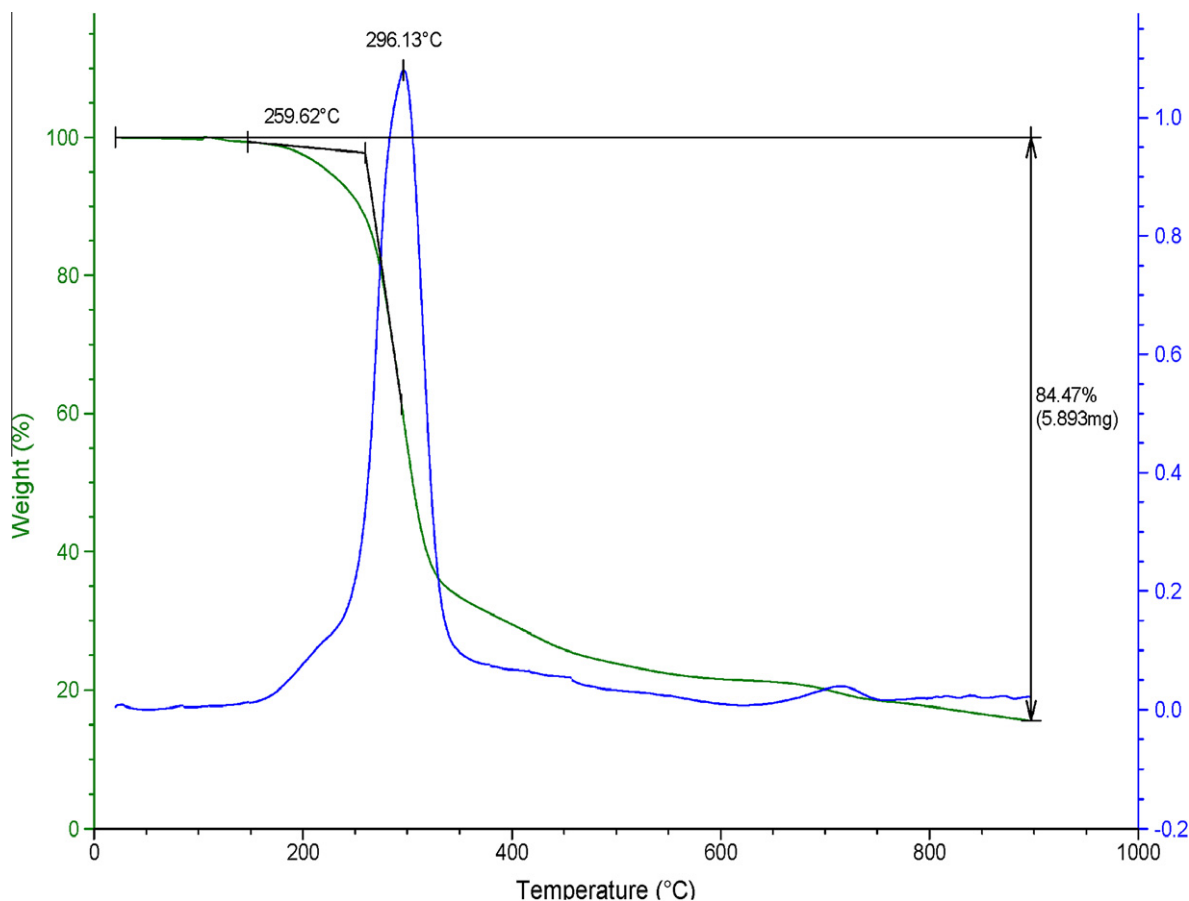**Fig. 5.** FAB-MS spectrum of complex $2L_1$.

Fig. 6. Fragmentation path of the first three stable fragments belongs to $2L_1$.

Fig. 7. IR-KBr disk spectrum of complex **2L₂**.

Fig. 8. TG and DTA thermal curves of complex **2L₁**.

Thermal studies

The thermal decomposition studies of the **2L₁–2L₃** complexes were investigated in the 25–900 °C temperature range under open atmosphere at a heating rate of 10 °C/min. All the **2L₁–2L₃** com-

plexes revealed a similar thermal behavior. Typical thermal TG and DTA curves of **2L₁** complex were given in Fig. 8. There is no weight loss in the range 25–260 °C which indicates the absence of coordinated or uncoordinated water molecule. Such complexes undergo one step decomposition with weight loss experimentally
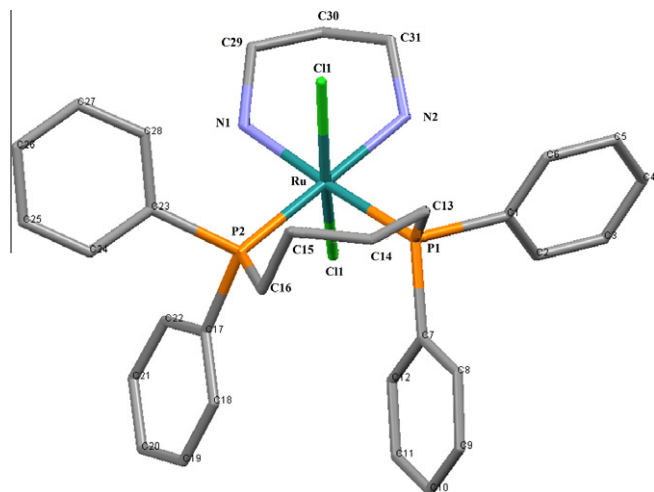
Fig. 9. Labeled ORTEP diagram of **2L₁** complex with thermal probability. All hydrogen atoms were omitted for clarity.
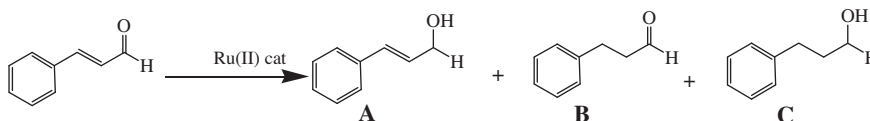
Table 2
Selected bond lengths (Å) and angles (°) for **2L₁**.

Ru(1)–Cl(1)	2.4161(6)
Ru(1)–Cl(2)	2.4299(6)
Ru(1)–N(1)	2.1994(19)
Ru(1)–N(2)	2.2030(2)
Ru(1)–P(1)	2.2943(6)
Ru(1)–P(2)	2.2842(6)
Cl(1)–Ru(1)–Cl(2)	163.82(2)
N(1)–Ru(1)–N(2)	85.36(11)
P(2)–Ru(1)–P(1)	90.19(2)
N(1)–Ru(1)–P(2)	92.94(9)
N(2)–Ru(1)–P(2)	177.41(7)
N(1)–Ru(1)–P(1)	176.87(10)
N(2)–Ru(1)–P(1)	91.51(6)
N(1)–Ru(1)–Cl(1)	88.05(6)
N(2)–Ru(1)–Cl(1)	85.65(7)
P(2)–Ru(1)–Cl(1)	96.25(2)
P(1)–Ru(1)–Cl(1)	91.57(2)
N(1)–Ru(1)–Cl(2)	81.43(6)
N(2)–Ru(1)–Cl(2)	81.30(7)
P(2)–Ru(1)–Cl(2)	96.54(2)
P(1)–Ru(1)–Cl(2)	98.26(2)

85%, the coordinated chlorides, diamine, dppb ligands have been moved away from the complex in between 260 and 365 °C with exothermic DTA peaks at 296.13 °C. The final residue was analyzed by IR spectra and identified as ruthenium oxide (RuO).

X-ray structural analyses for complex (2L₁)

The molecular structure of the **2L₁** complex has been determined by single crystal X-ray diffraction and the ORTEP diagram is given in Fig. 9. The **2L₁** is crystallized as free solvated *trans*-dichloro-*cis*-(dppb)-*cis*-(diamine)ruthenium(II) isomer with approximate C_{2v} symmetry.

Table 3
Hydrogenation of Cinnamic aldehyde using **2L₁–2L₃** complexes.

Trial	Catalyst	Conversion (%)[a]	TOF[b]	Selectivity (%)[a]		
				A	B	C
1	**2L₁**	>99	920	>99	0	0
2	**2L₂**	96	905	>99	0	0
3	**2L₃**	42	520	>99	0	0
4	**2L₃**	88[c]	88	>99	0	0
5	**2L₁**	0[d]	0	0	0	0

[a] Yields and selectivities were determined by GC.
[b] TOF: turnover frequency ($mol_{sub}\ mol^{-1}_{cat}\ h^{-1}$).
[c] 10 h react.
[d] 20 h react, K_2CO_3 co-catalyst was investigated instead of KOH.

The crystal data and structural refinement of **2L₁** are summarized in Table 1. The selected bond distances and bond angles are given in Table 2.

The ruthenium atom is coordinated with two chlorine species in *trans* form, one diamine co-ligand *via* the nitrogen atoms and one dppb ligand *via* the phosphorus atoms in *cis* forms as in scheme 1. The coordination environment around the ruthenium center is slightly distorted octahedral in nature with two Ru–N distances of 2.199 and 2.203 Å, two Ru–Cl distances of 2.416 and 2.430 Å and two Ru–P distances equal to 2.294 and 2.284 Å. The diamine and diphosphine ligands are practically planar. The coordination angle of the diamine chelate ring results in distinctly N–Ru–N angle of 85.36° that departs from ideal value by up to approximately 4.6°, due to the six-membered ring chelating nature of 1,3-propanediamine ligand, while the P–Ru–P angle is equal to 90.19° with negligible deviation from ideality due to the seven-membered ring chelating nature of the dppb ligand. The dichloro ligands are bent away from their axial positions toward the diamine ligand forming Cl–Ru–Cl angle of 163.82° with 16° deviation, resonating to the steric effect of the phenyls in the phosphine ligands. In the crystal structure there are a number of RuCl···HN contacts smaller than 3.0 Å, indicating the presence of unconventional intra-hydrogen bonds [20,21].

Catalytic activity of complexes 2L₁–2L₃ in the hydrogenation of Cinnamic aldehyde

Ruthenium complexes with the formation of [RuCl₂(diphosphine)diamine] have been used as transfer hydrogen catalysts under H_2 atmosphere using strong base as co-catalyst and 2-propanol as solvent [2–7]. To evaluate the catalytic activity of the **2L₁–2L₃** complexes, Cinnamic aldehyde (*trans*-4-phenyl-3-propene-2-al) was selected, in order to determine the hydrogenation selectivity and activity of the desired complexes, three different rego-selective hydrogenation reactions are expected (Scheme 2).

The selective hydrogenation of the carbonyl group affords the corresponding unsaturated alcohol A. Unwanted and hence of minor interest both the hydrogenation of the C=C double bond B, leading to the full hydrogenation of C=O and C=C bonds C. The hydrogenation reactions using complexes **2L₁–2L₃** as catalysts were carried out under identical conditions: 40 °C with a molar substrate: catalyst (TON, S/C) ratio of 1000/1, under 3 bar of hydrogen
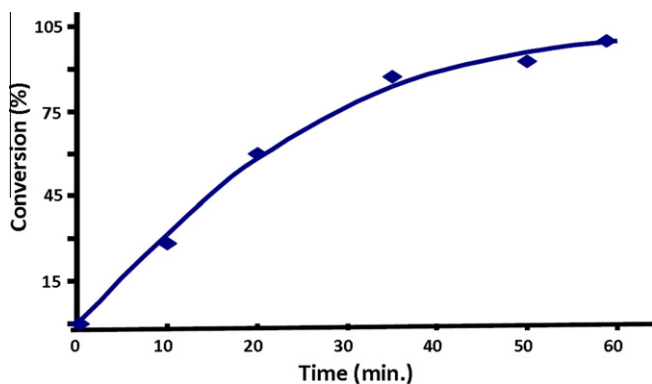

Scheme 2. Different catalytic hydrogenation possibilities of Cinnamic aldehyde.

Fig. 10. Hydrogenation reaction of Cinnamic aldehyde using **2L₁** under above mild condition.

pressure, in 40 ml of 2-propanol [Ru: Co-catalysts (KOH or K_2CO_3): Cinnamic aldehyde] [1:10:1000].

Data for the reduction of Cinnamic aldehyde to *trans*-4-phenyl-3-propene-2-ol are illustrated in Table 3.

The hydrogenation reactions under the above condition using complexes **2L₁** and **2L₂** as catalyst were finished within 1–2 h which enhanced the TOF number. Complex **2L₃** was slightly less active under identical condition compared to complex **2L₁** and **2L₂** which can be attributed to less stability of seven diamine ring formed. These catalysts were only effective in the presence of excess hydrogen in 2-propanol and a strong basic co-catalyst like KOH, when K_2CO_3 weak base was served as co-catalyst, no hydrogenation reaction was observed even if the reaction was lifted for longer time. Reduction of C=C bond in Cinnamic aldehyde was not detected at all and the hydrogenation of C=O bond selectivity reached up 99%.

The GC-conversion of the hydrogenation process using **2L₁** was plotted vs. reaction time per minutes (Fig. 10).

Conclusions

Complexes of type $Cl_2Ru(dppb)$diamine **2L₁**–**2L₃** using three types of diamine were prepared and characterized on the basis of EA, IR, UV–Vis, ^1H, ^{13}C and $^{31}P\{^1H\}$NMR and FAB-MS, TG/DTA and X-ray single crystal measurement. In solid state using X-ray single crystal the structure of **2L₁** characterized as *trans*-$Cl_2Ru(dppb)$diamine isomer, was confirmed by liguid $^{31}P\{^1H\}$NMR.

The desired complexes are proved to be catalytically very active and excellent in selective C=O hydrogenation over C=C of Cinnamic aldehyde under basic mild conditions.

Supplementary material

Crystallographic data have been deposited with the Cambridge Crystallographic Data Centre as supplementary publication num-ber CCDC 781815. Copies of this information may be obtained free of charge via www.ccdc.cam.ac.uk/conts/retrieving.html (or from the CCDC, 12 Union Road, Cambridge CB2 1EZ, UK; fax: +44 1223 336033; e-mail: deposit@ccdc.cam.ac.uk).

References

[1] N. Shan, H. Adams, J.A. Thomas, Inorg. Chim. Acta 358 (2005) 3377.
[2] I. Warad, E. Lindner, K. Eichele, H.A. Mayor, Inorg. Chim. Acta 357 (2004) 1847–1853.
[3] E. Lindner, I. Warad, K. Eichele, H.A. Mayor, Inorg. Chim. Acta 350 (2003) 49–56.
[4] C.D. Gilheany, M.C. Mitchell, in: F.R. Hartley (Ed.), The Chemistry of Organophosphorus Compounds, Wiley and Sons, New York, 1990.
[5] R. Noyori, Asymmetric Catalysis in Organic Synthesis, Wiley and Sons, New York, 1994.
[6] R. Noyori, T. Ohkuma, Angew. Chem. Int. Ed. 40 (2001) 40–120.
[7] E. Lindner, H.A. Mayor, I. Warad, K. Eichele, J. Organomet. Chem. 665 (2003) 176–185.
[8] I. Warad, M. Azam, U. Karama, S. Al-Resayes, A. Aouissi, B. Hammouti, J. Mol. Struct. 1002 (2011) 107–112.
[9] I. Warad, M.R. Siddiqi, S. Al-Resayes, A. Al-Warthan, R. Mahfouz, Trans. Met. Chem. 34 (2009) 337–352.
[10] K. Abdur-Rashid, M. Faatz, J.A. Lough, R.H. Morris, J. Am. Chem. Soc. 123 (2001) 7473–7474.
[11] M. Kitamura, M. Tounaga, T. Ohkuma, R. Noyori, Tetrahedron Lett. 32 (1991) 4163–4168.
[12] J.-X. Gao, T. Ikariya, R. Noyori, Organometallics 15 (1996) 1087–1089.
[13] G.A. Grasa, A. Zanotti-Gerosa, J.A. Medlock, W.P. Hems, Org. Lett. 7 (2005) 1449–1451.
[14] I. Warad, Molecules 15 (2010) 4652–4661.
[15] J.A. Moss, J.C. Yong, J.M. Stipkala, X.-G. Wen, C.A. Bignozzi, G.J. Meyer, T.J. Meyer, Inorg. Chem. 43 (2004) 1784–1792.
[16] T.J. Meyer, H.V. Huynh, Inorg. Chem. 42 (2003) 8140–8160.
[17] P. Kumar, A.K. Singh, M. Yadav, P.-z. Li, S.K. Singh, Q. Xu, D.Sh. Pandey, Inorg. Chim. Acta 368 (2011) 124–131.
[18] S.E. Clapham, A. Hadyovic, R.H. Morris, Coord. Chem. Rev. 248 (2004) 2201–2248.
[19] N. Chitrapriya, T.S. Kamatchi, M. Zeller, H. Lee, K. Natarajan, Spectrochim. Acta A 81 (2011) 128–134.
[20] I. Warad, Z. Kristallogr. New Cryst. Struct. 222 (2007) 415–417.
[21] M.A. Khanfar, I. Warad, M.A. Al-Damen, Acta Cryst. E66 (2010) 731.
[22] T.A. Stephenson, G. Wilkinson, J. Inorg. Nucl. Chem. 28 (1966) 945–956.
[23] G.M. Sheldrick, SHELXS-90, University of Gottingen, Gottingen, Germany, 1990.
[24] G.M. Sheldrick, SHELXS-97, University of Gottingen, Gottingen, Germany, 1997.
[25] A.A. Batista, M.O. Santiago, C.L. Donnici, I.S. Moreira, P.C. Healy, S.J. Berners-Price, S.L. Queiroz, Polyhedron 20 (2001) 2123–2128.
[26] S.L. Queiroz, A.A. Batista, G. Oliva, M.T. Gambardella, R.H. Santos, K.S. MacFarlane, S.J. Rettig, B.R. James, Inorg. Chim. Acta 267 (1998) 209–221.
[27] M.O. Santiago, J.R. Sousa, I.C. Diogenes, L.G. Lopes, E. Meyer, E.E. Castellano, J. Ellena, A.A. Batista, I.S. Moreira, Polyhedron 25 (2006) 1543–1548.